

Enhancement of electromechanical properties in lead-free (1-x)K_{0.5}Na_{0.5}O₃-xBaZrO₃ piezoceramics

Trang An Duong¹, Hoang Thien Khoi Nguyen¹, Sang-Sub Lee¹, Chang Won Ahn²,
Byeong Woo Kim³, Jae-Shin Lee¹, and Hyoung-Su Han^{1,*}

Abstract

This study analyzes the phase transition behavior and electrical properties of lead-free (1-x)K_{0.5}Na_{0.5}NbO₃-xBaZrO₃ (KNN-100xBZ) piezoelectric ceramics. The stabilized crystal structures in BaZrO₃-modified KNN ceramics is clarified to be pseudocubic. The polymorphic phase transition from the orthorhombic to pseudocubic phases can be observed with KNN-6BZ ceramics considering the optimized piezoelectric constant (d_{33}). Electromechanical strain behaviors are discussed. Accordingly, the enhancement of strain value at $x = 0.08$ (composition) may originate from the coexistence of ferroelectric domains and polar nanoregions. A schematic of domains for KNN, KNN-8BZ, and KNN-15BZ ceramics has been proposed to describe the relationship between the stabilized relaxor and changes in electrical properties.

Keywords : Lead-free, Piezoceramics, Relaxor, PNRs, Phase transition.

1. INTRODUCTION

Lead-based piezoceramics with efficient electrical properties, e.g., Pb(Zr_{0.52}Ti_{0.48})O₃ (PZT), Pb(Mg_{1/3}Nb_{2/3})O₃-PbTiO₃ (PMN-PT) [1], and (Pb,La)(Zr,Ti)O₃ (PLZT) [2], are widely applied to electronic and electrical devices. However, these materials contain lead (>60%) as a classifiable toxicity, which severely affects human and environment [3]. In recent times, several scientists focused on the development of lead-free piezoceramics to replace lead-based materials [4-6].

Among lead-free piezoelectric materials, K_{0.5}Na_{0.5}NbO₃ (KNN) and its compounds are promising candidates owing to their excellent dielectric and piezoelectric properties [7,8]. Several studies have been carried out to improve electrical properties for KNN-based materials based on concept of polymorphic phase

transition (PPT) [9]. Although electrical properties of KNN-based materials can be improved based the PPT concept, temperature sensitivity issue remains a challenge. To overcome this problem, there are several methods, such as texturing, stabilization of a single tetragonal phase, and formation of a morphotropic phase boundary (MPB) like that of PZT [10,11]. Although texturing in ceramics can exhibit high piezoelectric performance and excellent temperature stability [12,13], it requires complex synthesis process with a high cost. In the case of the stabilization of a single tetragonal phase, thermal sensitivity improves, while piezoelectric properties degrade [14,15]. Hence, the MPB concept with thermal stability and a high piezoelectric property would be the most promising approach.

To form MPB, two phases, c tetragonal (T) phase and rhombohedral (R) phase, are required to be stabilized simultaneously [16]. Several candidates can help stabilization T phase at room temperature in the KNN-based system [17-20], while the R phase at room temperature is relatively rare. The reason for this is that the R phase is inherently stabilized at a low temperature (around -120 °C) in KNN ceramics. It implies that the R phase in KNN would be difficult to stabilize near room temperature. Nevertheless, few studies have claimed that the modification of zirconium-based compounds (especially BaZrO₃) in KNN ceramics can help stabilize the R phase near room temperature [21,22]. In 2009, Wang *et al* first reported the induced R phases by modifying BaZrO₃ (BZ) [21] and other AZrO₃ [22] in KNN ceramics. Then, several studies have reported the formation of

¹ School of Materials Science and Engineering, University of Ulsan, 12, Techno saneop-ro 55 beon-gil, Nam-gu, Ulsan 44776, Republic of Korea

² Department of Physics and EHSRC, University of Ulsan, 93, Daehak-ro, Nam-gu, Ulsan 44610, Republic of Korea

³ Department of Electrical Engineering, University of Ulsan, 93, Daehak-ro, Nam-gu, Ulsan 44610, Republic of Korea

*Corresponding author: hsejs@ulsan.ac.kr

(Received: Oct. 15, 2021, Revised: Nov. 25, 2021, Accepted: Nov. 30, 2021)

This is an Open Access article distributed under the terms of the Creative Commons Attribution Non-Commercial License(<https://creativecommons.org/licenses/by-nc/3.0/>) which permits unrestricted non-commercial use, distribution, and reproduction in any medium, provided the original work is properly cited.

MPB (comprising R and T phases) in KNN-based ceramics using zirconium-based compounds [23,24]. On the other hand, it has been recently suggested that relaxor behavior relating to the phase boundary between an orthorhombic or tetragonal phase and cubic phase (pseudocubic) phase in KNN-based ceramics can help enhance electrical properties [25-28]. Accordingly, this implies that the identity of stabilized phase in KNN-based ceramics is still a highly controversial issue. Furthermore, the investigation on electromechanical strain behaviors with temperature stability in KNN-based ceramics remains a challenge.

Therefore, this study investigated the effect of modified BZ on crystal structures, phase transition behaviors, and electrical properties in KNN ceramics. Furthermore, we have successfully demonstrated the modeling for enhanced electromechanical strain properties in BZ-modified KNN ceramics by comparing virgin strain curves (e.g., poling strain curves) between pure KNN and BZ-modified KNN ceramics.

2. EXPERIMENTAL

Lead-free piezoelectric $(1-x)(\text{Na}_{0.5}\text{K}_{0.5})\text{NbO}_3-x\text{BaZrO}_3$ (KNN-100xBZ; $x=0.03, 0.06, 0.08, 0.10,$ and 0.15) ceramics were prepared using a conventional solid-state reaction method. High-purity carbonate powders, e.g., Na_2CO_3 (99%), K_2CO_3 (99%), and BaCO_3 (99.95%), and oxide powders, e.g., Nb_2O_5 (99.9%) and ZrO_2 (98%), were used as raw materials. After being mixed in stoichiometric proportions based on the conventional ball-milling method in ethanol using Zirconia balls, the mixtures were dried and calcined at 850°C for 3 h to form uniform solid solutions. The calcined powders were mixed with polyvinyl alcohol (PVA) as a binder, pressed into green body discs of diameter 12 mm under a uniaxial pressure of 200 MPa, and sintered at $1110\text{--}1220^\circ\text{C}$ for 3 h.

The crystal structures of all the samples were characterized by means of X-ray diffractometry (XRD, RAD III, Rigaku, Japan), and microstructures were observed using field-emission scanning electron microscopy (FE-SEM, JEOL JSM-6500F, Japan). The silver paste was applied to both sides of each specimen and baked at 700°C for 30 min to form an electrode on the samples for electrical measurements. The temperature-dependent dielectric constant and dielectric loss were recorded using a high-temperature electric prober system (KEYSIGHT-E4980AL Precision LCR Meter, USA). The piezoelectric constant (d_{33}) was measured using a quasistatic piezoelectric d_{33}/d_{31} meter (ZJ-6B; Institute of Acoustics, Chinese Academy of Sciences, Beijing, China). Electric-field-induced strain (S) curves and polarization

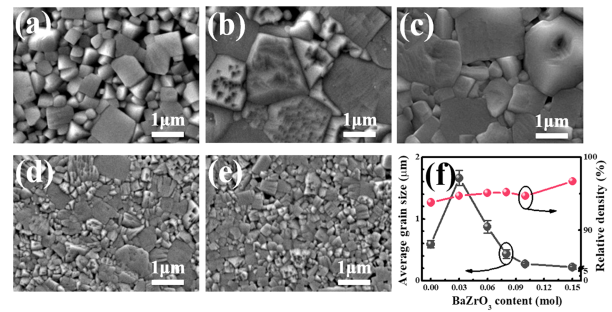


Fig. 1. Polished and thermally etched surface images of KNN-100xBZ ceramics: (a) $x = 0$, (b) $x = 0.03$, (c) $x = 0.06$, (d) $x = 0.08$, (e) $x = 0.10$, and (f) the calculated average grain size and relative density values of KNN-100xBZ ceramics as a function of BZ content.

(P) curves of the electric field (E) were measured at 1 Hz using aixPES (aixACCT Systems GmbH, Germany).

3. RESULTS AND DISCUSSIONS

Fig. 1 shows the polished and thermally etched surface images of KNN-100xBZ ceramics. All the samples exhibited dense microstructures with very small numbers of holes and inhomogeneous grain distributions. We obtained that the relative density of KNN-100xBZ ceramics monotonically improved with an increase in the BZ content. This result indicates the improved sinterability of KNN ceramics by modifying BZ, which is compared in Fig. 1. The average grain size increased from 0.61 ± 0.02 mm for pure KNN to the highest value of 1.67 ± 0.04 mm for KNN-3BZ. It is suggested that low concentrations of BZ can be well diffused into KNN lattices to form a new homogeneous solid solution, responsible for grain growth [29,30]. However, the average grain size has drastically decreased with a further increase in the BZ content. This implies that excess particles of BZ at high concentrations may remain near the grain boundary and restrain the grain growth [31-33].

Fig. 2 shows XRD patterns for BZ-modified KNN ceramics. Peaks in 2θ ranges of $30.3^\circ\text{--}32.5^\circ$, $43.7^\circ\text{--}46.5^\circ$, and $55.2^\circ\text{--}57.4^\circ$ are investigated to clarify changes in crystal structure for all compositions. As shown in Fig. 2(b), two distinct peaks as (202) and (020) are observed in pure KNN and KNN-3BZ ceramics that correspond to a single orthorhombic structure. For KNN-6BZ ceramics, the split peaks began transitioning into (200) peak. At KNN-8BZ ceramics, the peaks are merged into a single (200) peak corresponding to a rhombohedral or a cubic structure.

In fact, ($h00$), ($hh0$), and (hhh) reflections of cubic symmetry

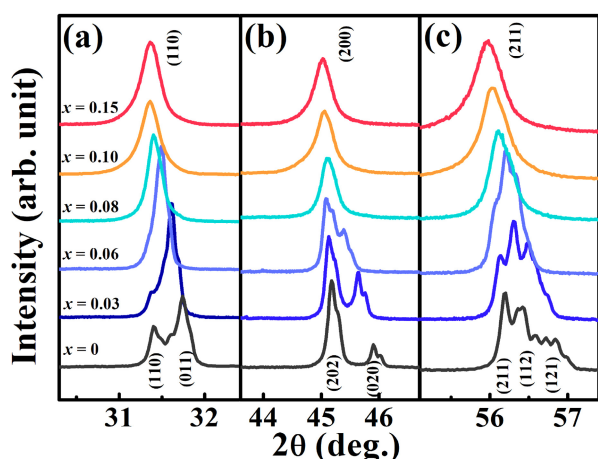


Fig. 2. X-ray diffraction patterns of KNN-100xBZ ceramics as a function of the BZ content in the 2θ ranges of (a) 30.3°–32.5°, (b) 43.7°–46.5°, and (c) 55.2°–57.4°.

are reflected as single peaks based on the perpendicularity. Meanwhile, a rhombohedral symmetry ($\alpha = \beta = \gamma \neq 90^\circ$) indicates split peaks at ($hh0$) and (hhh) reflections [34, 35]. Accordingly, KNN-8BZ ceramics can be identified as a cubic structure by detecting single (110) peaks in Fig. 2 (a) and single (211) peaks in Fig. 2 (c).

Fig. 3 shows the temperature-dependent dielectric properties of KNN-100xBZ ceramics. Curie temperature (T_C) and temperature with regard to an orthorhombic to a tetragonal phase transition (T_{O-T}) were decreased with an increase in the BZ content. T_C monotonically reduced from 400 °C for pure KNN to 60 °C for KNN-15BZ ceramics, while T_{O-T} reduced from 200 °C for KNN to near room temperature for KNN-8BZ ceramics. We observed sharp phase transitions (first-order phase transition behaviors) in pure KNN, KNN-3BZ, and KNN-6BZ ceramics that these

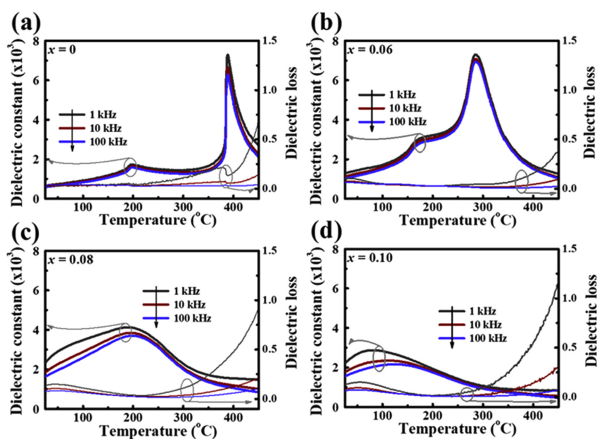


Fig. 3. Temperature-dependent dielectric constant for KNN-100xBZ ceramics as a function of BZ content.

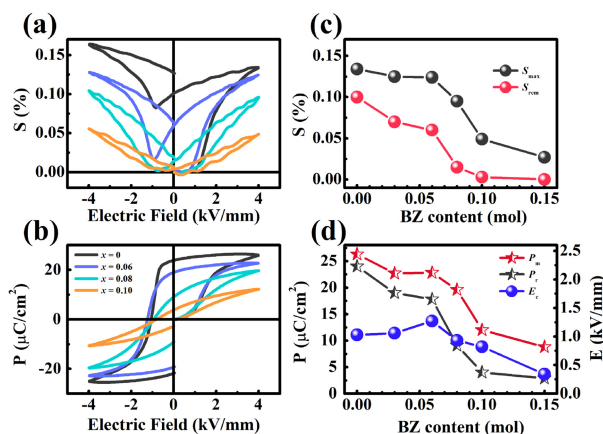


Fig. 4. (a) Bipolar strain ($S-E$) and (b) polarization ($P-E$) curves and extracted parameters such as (c) S_{max} , S_{rem} and (d) P_{max} , P_r , E_c for KNN-100xBZ ceramics as a function of the BZ content.

features can be categorized as normal ferroelectrics.

On the other hand, frequency-dependent dielectric behaviors with a broad phase transition as a function of the applied frequency were observed in KNN-8BZ ceramics, and became stronger dispersion with further increasing BZ content. BZ modification in KNN ceramics significantly affects dielectric properties and is responsible for ferroelectrics to relaxor phase transition.

Electromechanical strain ($S-E$) and polarization ($P-E$) curves for KNN-100xBZ ceramics as a function of BZ content are compared in Fig. 4. At BZ content $x < 0.08$, typical ferroelectric features such as butterfly-shaped $S-E$ curves and square-shaped $P-E$ curves were observed. On the other hand, the significantly reduced remnant polarization (P_r) and the negligible remanent strain (S_{rem}) can be observed for KNN-10BZ and KNN-15BZ ceramics. In the case of coercive field (E_c), first, it was monotonically increased and drastically decreased with an increase in the BZ content. The highest maximum strain (S_{max}) was obtained at KNN-8BZ ceramics with a drastic decrease in P_r and remanent strain (S_{rem}). Changes in those results are strongly related to the appearance of relaxor features in KNN-100xBZ ceramics [28,36]. It will be discussed in detail with a phase diagram (in Fig. 5) and a schematic modeling for strain mechanism (in Fig. 6).

Fig. 5 shows a phase diagram based on crystallographic changes and electrical properties for KNN-100xBZ ceramics as a function of the BZ content. The piezoelectric constant (d_{33}) slightly increased with an increase in the BZ content up to 6 mol% and then drastically declined with a further increase in the BZ content. The highest value of d_{33} of 130 pC/N was obtained in

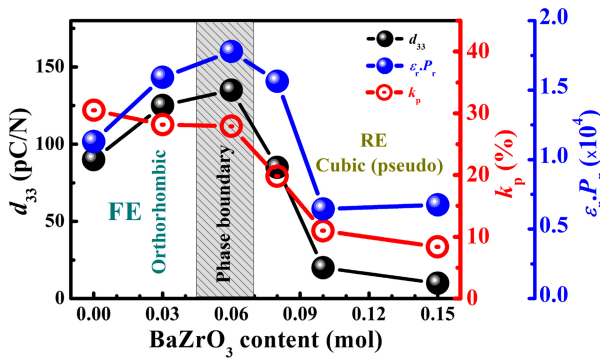


Fig. 5. Compositional phase diagram of KNN-100xBZ ceramics with changes in piezoelectric constant (d_{33}), electromechanical coupling factor (k_p), and $\epsilon_r \cdot P_r$ as a function of the BZ content.

KNN-6BZ ceramics, which may be related to the PPT concept with the coexistence of orthorhombic and cubic phases.

Several studies reported that these enhanced electrical properties in KNN-based ceramics originated from the coexistence of two phases corresponding to the polymorphic phase boundary [19,37]. In the case of the electromechanical coupling factor (k_p) for KNN-100xBZ ceramics, first, we observed a slight reduction of up to 6 mol% of BZ and then a drastic degradation with a further increase in the BZ content. Moreover, it is suggested that the BZ modification in KNN-based ceramics causes the dissociation of long-range-ordered ferroelectricity based on compositional disorder and lattice distortion [38-40]. Therefore, the destabilization of ferroelectrics with the stabilization of relaxor (cubic phase) is responsible for the drastic degradation of k_p and d_{33} for $x \geq 0.08$ composition. Moreover, changes in d_{33} for KNN-100xBZ ceramics are strongly influenced by the product of the dielectric constant (ϵ_r) and remanent polarization (P_r) [41], as expressed by the following equation:

$$d_{33} = 2Q\epsilon_r P_r, \quad (1)$$

where Q is the electrostrictive coefficient of materials. As a result, the corresponding trend of d_{33} and $\epsilon_r \times P_r$ graphs in Fig. 5 indicates that piezoelectric constant is well related to dielectric and ferroelectric properties.

For better understanding of the improved electromechanical strain properties in KNN-8BZ ceramics, schematic modeling of electromechanical strain behaviors of three different states was proposed (Fig. 6). In principle, the proposed schematic modeling includes normal ferroelectrics with ferroelectric domains (FDs) for pure KNN ceramics, a relaxor state with polar nanoregions

(PNRs) for KNN-15BZ ceramics, and an intermediate state with the coexistence of relaxor and ferroelectrics for KNN-8BZ ceramics.

At the initial state (i), all the compositions regardless of FDs and/or PNRs are randomly organized, which results in no microscopic polarization (corresponding to the zero point in strain curves). In the case of pure KNN ceramics shown in Fig. 6(a), the FDs can be aligned toward the applied electric field direction, which was expressed as state (ii) [42]. The most important feature in this state is accompanied by a huge strain—poling strain (S_{pol}). Once the domains are aligned, they no longer revert to initial state even if the applied electric field is removed, which corresponds to state (iii). Thus, huge remanent strain (S_{rem}) and polarization remain in normal ferroelectric materials. Therefore, usable strain corresponding to unipolar strain (S_{uni}) can be obtained in pure KNN ceramics as normal ferroelectrics. In fact, S_{uni} can be expressed by the difference of $S_{pol} - S_{rem}$ [43,44].

In contrast, it is suggested that KNN-15BZ ceramics is expressed as a relaxor state with dynamic PNRs (Fig. 6(c)). In this case, all the PNRs can easily align along the electric field direction. However, it is impossible to induce long-range-ordered or macroscopic ferroelectric domains owing to insufficient interaction among PNRs (their size and numbers). Therefore, low S_{pol} was obtained in KNN-15BZ ceramics. When the applied electric field is removed ($E = 0$, as state (iii)), the aligned PNRs rapidly revert to the initial state (state (i)) as a randomized configuration, thereby resulting in negligible S_{rem} .

As we explained previously, the coexistence of PNRs and FDs was suggested in KNN-8BZ ceramics (Fig. 6(b)). Once a

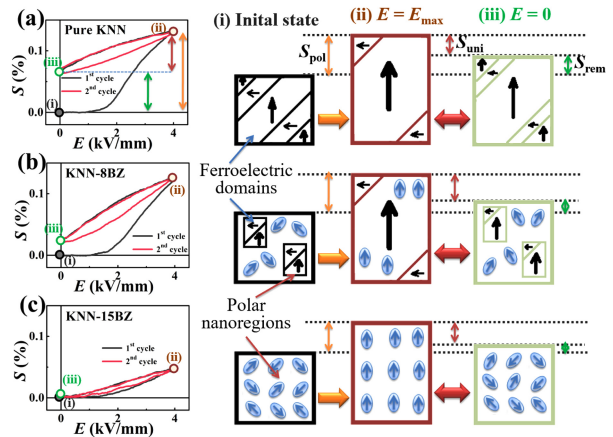


Fig. 6. Modeling of electromechanical strain of three different states: (a) normal ferroelectrics (pure KNN ceramics), (b) an intermediate state with coexistence of PNRs and ferroelectric domains (KNN-8BZ ceramics), and (c) relaxor state with PNRs (KNN-15BZ ceramics).

significant electric field is applied (corresponding to state (ii)), PNRs and FDs are sequentially reoriented along the applied electric field direction. In this case, it is expected that most relaxor regions (nonpolar phase) are reversibly transformed into the long-range-ordered ferroelectric domains. Therefore, S_{pol} (corresponding to S_{max}) of KNN-8BZ ceramics is compared with that of pure KNN ceramics. PNRs with FDs play an important role in reducing the energy barrier related to the domain switching in KNN-8BZ ceramics as “accelerators” [45]. The most important feature of KNN-8BZ ceramics is that S_{rem} drastically reduces as state (iii). When the applied electric field is removed, induced ferroelectric domains mostly revert to the initial state. This result implies that the reversible transition from relaxor to ferroelectric domains is responsible for the optimized S_{pol} and minimized S_{rem} in KNN-8BZ ceramics. Based on the relationship of $S_{\text{uni}} \approx S_{\text{pol}} - S_{\text{rem}}$, significantly enhanced electromechanical strain is obtained in KNN-8BZ ceramics.

4. CONCLUSIONS

Lead-free KNN-100xBZ piezoelectric ceramics were successfully prepared using a conventional solid-state reaction method. According to single peaks at (110) and (211) reflections in XRD pattern, the stabilized crystal structures in BaZrO₃-modified KNN ceramics can be identified as the cubic (pseudocubic) phase. The polymorphic phase transition from the ferroelectric orthorhombic phase to the relaxor cubic phase was observed in KNN-6BZ ceramics with the optimized piezoelectric constant d_{33} . Moreover, we found and suggested that the enhanced electromechanical strain in KNN-8BZ ceramics is originated from the coexistence of FDs and PNRs. Furthermore, to explain the enhanced electromechanical strain properties, a schematic related to domain structures of KNN-100xBZ ceramics was successfully illustrated using virgin unipolar strain curves as a function of electric field.

ACKNOWLEDGMENT

This study was supported by the National Research Foundation (NRF) of the Republic of Korea (Grant Nos. 2020R1C1C1007375 and 2016R1D1A3B01008169). CW Ahn acknowledges financial support from the Basic Science Research Program through the National Research Foundation (NRF) of the Republic of Korea (Grant No. 2021R111A1A01057086).

REFERENCES

- [1] M. S. Islam and J. Beamish, “Piezoelectric creep in LiNbO₃, PMN-PT and PZT-5A at low temperatures”, *J. Appl. Phys.*, Vol. 126, No. 20, pp. 204101(1)-204101(12), 2019.
- [2] A. Kuma, A. K. Kalyani, R. Ranjan, K. C. J. Raju, J. Ryu, N. Park, and A. R. James, “Evidence of monoclinic phase and its variation with temperature at morphotropic phase boundary of PLZT ceramics”, *J. Alloys Compd.*, Vol. 816, pp. 152613(1)-152613(10), 2020.
- [3] A. J. Bell and O. Deubzer, “Lead-free piezoelectrics—The environmental and regulatory issues”, *MRS Bull.*, Vol. 43, No. 8, pp. 581-587, 2018.
- [4] C. H. Hong, H. P. Kim, B. Y. Choi, H. S. Han, J. S. Son, C. W. Ahn, and W. Jo, “Lead-free piezoceramics – Where to move on?”, *J. Mater.*, Vol. 2, No. 1, pp. 1-24, 2016.
- [5] M. Arshad, H. Du, M. Javed, A. Maqsood, I. Ashraf, H. Sussain, W. Ma, and H. Ran, “Fabrication, structure, and frequency-dependent electrical and dielectric properties of Sr-doped BaTiO₃ ceramics”, *Ceram. Int.*, Vol. 46, No. 2, pp. 2238-2246, 2020.
- [6] T. A. Duong, H. S. Han, Y. H. Hong, Y. S. Park, H. T. K. Nguyen, T. H. Dinh, and J. S. Lee, “Dielectric and piezoelectric properties of Bi_{1/2}Na_{1/2}TiO₃-SrTiO₃ lead-free ceramics”, *J. Electroceram.*, Vol. 41, No. 1, pp. 73-79, 2018.
- [7] J. Wu, D. Xiao, and J. Zhu, “Potassium-sodium niobate lead-free piezoelectric materials: past, present, and future of phase boundaries”, *Chem. Rev.*, Vol. 115, No. 7, pp. 2559-2595, 2015.
- [8] J. F. Li, K. Wang, F. Y. Zhu, L. Q. Cheng, F. Z. Yao, and D. J. Green, “(K,Na)NbO₃-based lead-free piezoceramics: fundamental aspects, processing technologies, and remaining challenges”, *J. Am. Ceram. Soc.*, Vol. 96, No. 12, pp. 3677-3696, 2013.
- [9] I. Izzuddin, M. H. Hj. Jumal, Z. Zainuddin, and N. H. Janil, “Piezoelectric enhancements in K_{0.5}Na_{0.5}NbO₃-based ceramics via structural evolutions”, *Ceram. Int.*, Vol. 45, No. 14, pp. 17204-17209, 2019.
- [10] X. Lv, J. Wu, and X. Zhang, “A new concept to enhance piezoelectricity and temperature stability in KNN ceramics”, *Chem. Eng. J.*, Vol. 402, pp. 126215(1)-126215(12), 2020.
- [11] W. Yang, P. Li, S. Wu, F. Li, B. Shen, and J. Zhai, “Coexistence of excellent piezoelectric performance and thermal stability in KNN-based lead-free piezoelectric ceramics”, *Ceram. Int.*, Vol. 46, No. 2, pp. 1390-1395, 2020.
- [12] Y. Chang, S. Poterala, Z. Yang, and G. L. Messing, “Enhanced electromechanical properties and temperature stability of textured (K_{0.5}Na_{0.5})NbO₃-based piezoelectric ceramics”, *J. Am. Ceram. Soc.*, Vol. 94, No. 8, pp. 2494-2498, 2011.
- [13] H. Zhang, Y. Zhu, P. Fan, M. A. Marwat, W. Ma, K. Liu, H. Liu, B. Xie, K. Wang, and J. Koruza, “Temperature-insensitive electric-field-induced strain and enhanced piezoelectric properties of <001> textured (K,Na)NbO₃-based lead-free piezoceramics”, *Acta Mater.*, Vol. 156, pp. 389-398, 2018.

- [14] S. Zhang, R. Xia, and T. R. Shrout, "Modified $(\text{K}_{0.5}\text{Na}_{0.5})\text{NbO}_3$ based lead-free piezoelectrics with broad temperature usage range", *Appl. Phys. Lett.*, Vol. 91, No. 13, pp. 132913(1)-132913(3), 2007.
- [15] L. Jiang, Y. Li, L. Xie, J. Wu, Q. Chen, W. Zhang, D. Xiao, and J. Zhu, "Enhanced electrical properties and good thermal stability in $\text{K}_{0.48}\text{Na}_{0.52}\text{NbO}_3\text{-LiNbO}_3\text{-BiAlO}_3$ lead-free piezoceramics", *J. Mater. Sci.: Mater. Electron.*, Vol. 28, No. 12, pp. 8500-8509, 2017.
- [16] H. Shi, J. Chen, R. Wang, and S. Dong, "Full set of material constants of $(\text{Na}_{0.5}\text{K}_{0.5})\text{NbO}_3\text{-BaZrO}_3\text{-(Bi}_{0.5}\text{Li}_{0.5})\text{TiO}_3$ lead-free piezoelectric ceramics at the morphotropic phase boundary", *J. Alloys Compd.*, Vol. 655, pp. 290-295, 2016.
- [17] Y. Guo, K. I. Kakimoto, and H. Ohsato, "Dielectric and piezoelectric properties of lead-free $(\text{Na}_{0.5}\text{K}_{0.5})\text{NbO}_3\text{-SrTiO}_3$ ceramics", *Solid State Commun.*, Vol. 129, No. 5, pp. 279-284, 2004.
- [18] Y. Guo, K. I. Kakimoto, and H. Ohsato, " $(\text{Na}_{0.5}\text{K}_{0.5})\text{NbO}_3\text{-LiTaO}_3$ lead-free piezoelectric ceramics", *Mater. Lett.*, Vol. 59, No. 2-3, pp. 241-244, 2005.
- [19] R. Wang, H. Bando, and M. Itoh, "Universality in phase diagram of $(\text{K},\text{Na})\text{NbO}_3\text{-MTiO}_3$ solid solutions", *Appl. Phys. Lett.*, Vol. 95, No. 9, pp. 092905(1)-092905(3), 2009.
- [20] H. Du, W. Zhou, F. Luo, D. Zhu, S. Qu, Y. Li, and Z. Pei, "Design and electrical properties' investigation of $(\text{K}_{0.5}\text{Na}_{0.5})\text{NbO}_3\text{-BiMeO}_3$ lead-free piezoelectric ceramics", *J. Appl. Phys.*, Vol. 104, No. 3, pp. 034104(1)-034104(7), 2008.
- [21] R. Wang, H. Bando, T. Katsumata, Y. Inaguma, H. Taniuchi, and M. Itoh, "Tuning the orthorhombic-rhombohedral phase transition temperature in sodium potassium niobate by incorporating barium zirconate", *Phys. Status Solidi Rapid Res. Lett.*, Vol. 3, No. 5, pp. 142-144, 2009.
- [22] R. Wang, H. Bando, M. Kidate, Y. Nishihara, and M. Itoh, "Effects of A-Site Ions on the Phase Transition Temperatures and Dielectric Properties of $(1-x)(\text{Na}_{0.5}\text{K}_{0.5})\text{NbO}_3\text{-xAZrO}_3$ Solid Solutions", *Jpn. J. Appl. Phys.*, Vol. 50, No. 9S2, pp. 09ND10(1)-09ND10(5), 2011.
- [23] Y. M. Li, Z. Y. Shen, F. Wu, T. Z. Pan, Z. M. Wang, and Z. G. Xiao, "Enhancement of piezoelectric properties and temperature stability by forming an MPB in KNN-based lead-free ceramics", *J. Mater. Sci. Mater. Electron.*, Vol. 25, No. 2, pp. 1028-1032, 2013.
- [24] T. A. Duong, F. Erkinov, H. T. K. Nguyen, C. W. Ahn, B. W. Kim, H. S. Han, and J. S. Lee, "Temperature insensitive piezoelectric properties on the morphotropic phase boundary of BaZrO_3 -modified lead-free KNN-BLT ceramics", *J. Electroceram.*, Vol. 45, No. 4, pp. 164-171, 2020.
- [25] V. Bobnar, J. Holc, M. Hrovat, and M. Kosec, "Relaxor-like dielectric dynamics in the lead-free $\text{K}_{0.5}\text{Na}_{0.5}\text{NbO}_3\text{-SrZrO}_3$ ceramic system", *J. Appl. Phys.*, Vol. 101, No. 7, pp. 074103(1)-074103(4), 2007.
- [26] Z. Liu, H. Fan, Y. Zhao, G. Dong, and W. Jo, "Optical and Tunable Dielectric Properties of $\text{K}_{0.5}\text{Na}_{0.5}\text{NbO}_3\text{-SrTiO}_3$ Ceramics", *J. Am. Ceram. Soc.*, Vol. 99, No. 1, pp. 146-151, 2016.
- [27] U. Nuraini, N. Triyuliana M. Mashuri, and S. Suasmoro, "Characterization of relaxor ferroelectrics from BiFeO_3 doped $(\text{K}_{0.5}\text{Na}_{0.5})\text{NbO}_3$ systems", *Mater. Sci. Eng.*, Vol. 496, No. 1, pp. 012043(1)-012043(6), 2019.
- [28] J. Zhou, G. Xiang, J. Shen, H. Zhang, Z. Xu, H. Li, P. Ma, and W. Chen, "Composition-insensitive enhanced piezoelectric properties in SrZrO_3 modified $(\text{K}, \text{Na})\text{NbO}_3$ -based lead-free ceramics", *J. Electroceram.*, Vol. 44, No. 1, pp. 95-103, 2019.
- [29] J. Du, Z. Xu, R. Chu, J. Hao, W. Li, and P. Zheng, "Enhanced electrical properties of lead-free $(1-x)(\text{K}_{0.44}\text{Na}_{0.52}\text{Li}_{0.04})(\text{Nb}_{0.91}\text{Ta}_{0.05}\text{Sb}_{0.04})\text{O}_3\text{-xSrZrO}_3$ ceramics", *J. Mater. Sci.: Mater. Electron.*, Vol. 27, No. 6, pp. 6535-6541, 2016.
- [30] W. Liang, W. Wu, D. Xiao, J. Zhu, and J. Wu, "Construction of new morphotropic phase boundary in $0.94(\text{K}_{0.4-x}\text{Na}_{0.6}\text{Ba}_x\text{Nb}_{1-x}\text{Zr}_x)\text{O}_3\text{-}0.06\text{LiSbO}_3$ lead-free piezoelectric ceramics", *J. Mater. Sci.*, Vol. 46, No. 21, pp. 6871-6876, 2011.
- [31] B. Zhang, J. Wu, X. Wang, X. Cheng, J. Zhu, and D. Xiao, "Rhombohedral-orthorhombic phase coexistence and electrical properties of Ta and BaZrO_3 co-modified $(\text{K}, \text{Na})\text{NbO}_3$ lead-free ceramics", *Curr. Appl. Phys.*, Vol. 13, No. 8, pp. 1647-1650, 2013.
- [32] J. Hao, Z. Xu, R. Chu, W. Li, and J. Du, "Effect of $(\text{Bi}_{0.5}\text{K}_{0.5})\text{TiO}_3$ on the electrical properties, thermal and fatigue behavior of $(\text{K}_{0.5}\text{Na}_{0.5})\text{NbO}_3$ -based lead-free piezoelectrics", *J. Mater. Res.*, Vol. 30, No. 13, pp. 2018-2029, 2015.
- [33] K. Ramam and M. Lopez, "Barium modified lead lanthanum strontium zirconium niobium titanate for dielectric and piezoelectric properties", *J. Eur. Ceram. Soc.*, Vol. 27, No. 10, pp. 3141-3147, 2007.
- [34] R. Guo, L. E. Cross, S. E. Park, B. Noheda, D. E. Cox, and G. Shirane, "Origin of the High Piezoelectric Response in $\text{PbZr}_{1-x}\text{Ti}_x\text{O}_3$ ", *Phys. Rev. Lett.*, Vol. 84, No. 23, pp. 5423-5426, 2000.
- [35] J. Fu, R. Zuo, S. C. Wu, J. Z. Jiang, L. Li, T. Y. Yang, X. Wang, and L. Li, "Electric field induced intermediate phase and polarization rotation path in alkaline niobate based piezoceramics close to the rhombohedral and tetragonal phase boundary", *Appl. Phys. Lett.*, Vol. 100, No. 12, pp. 122902(1)-122902(5), 2012.
- [36] J. Zhang, Z. Liu, T. Zhang, Y. Liu, and Y. Lyu, "High strain response and low hysteresis in BaZrO_3 -modified KNN-based lead-free relaxor ceramics", *J. Mater. Sci. Mater. Electron.*, Vol. 32, pp. 16715-16725, 2021.
- [37] H. C. Thong, C. Zhao, Z. Zhou, C. F. Wu, Y. X. Liu, Z. Z. Du, J. F. Li, W. Gong, and K. Wang, "Technology transfer of lead-free $(\text{K}, \text{Na})\text{NbO}_3$ -based piezoelectric ceramics", *Mater. Today*, Vol. 29, pp. 37-48, 2019.
- [38] H. Yu and Z. G. Ye, "Dielectric properties and relaxor behavior of a new $(1-x)\text{BaTiO}_3\text{-xBiAlO}_3$ solid solution", *J. Appl. Phys.*, Vol. 103, Vol. 3, pp. 034114(1)-034114(5), 2008.
- [39] A. A. Bokov and Z. G. Ye, "Recent progress in relaxor ferroelectrics with perovskite structure", *J. Mater. Sci.*, Vol. 41, No. 1, pp. 31-52, 2006.
- [40] A. A. Bokov, B. J. Rodriguez, X. Zhao, J. H. Ko, S. Jesse, X. Long, W. Qu, T. H. Kim, J. D. Budai, A. N. Morozovska,

- and S. Kojima, "Compositional disorder, polar nanoregions and dipole dynamics in $\text{Pb}(\text{Mg}_{1/3}\text{Nb}_{2/3})\text{O}_3$ -based relaxor ferroelectrics", *Zeitschrift für Kristallographie*, Vol. 226, pp. 99-107, 2011.
- [41] F. Li, M. J. Cabral, B. Xu, Z. Cheng, E. C. Dickey, J. M. L. Beau, J. Wang, J. Luo, S. Taylor, W. Hackenberger, L. Bellaiche, Z. Xu, L. Q. Chen, T. R. Shrout, and S. Zhang, "Giant piezoelectricity of Sm-doped $\text{Pb}(\text{Mg}_{1/3}\text{Nb}_{2/3})\text{O}_3$ - PbTiO_3 single crystals", *Science*, Vol. 364, No. 6437, pp. 264-268, 2019.
- [42] Q. M. Zhang, W. Y. Pan, S. J. Jang, and L. E. Cross, "Domain wall excitations and their contributions to the weak signal response of doped lead zirconate titanate ceramics", *J. Appl. Phys.*, Vol. 64, No. 11, pp. 6445-6451, 1988.
- [43] K. Wang, F. Z. Yao, W. Jo, D. Gobeljic, V. V. Shvartsman, D. C. Lupascu, J. F. Li, and J. Rödel, "Temperature-Insensitive (K,Na) NbO_3 -Based Lead-Free Piezoactuator Ceramics", *Advanced Functional Materials*, Vol. 23, No. 33, pp. 4079-4086, 2013.
- [44] H. S. Han, W. Jo, J. K. Kang, C. W. Ahn, I. W. Kim, K. K. Ahn, and J. S. Lee, "Incipient piezoelectrics and electrostriction behavior in Sn-doped $\text{Bi}_{1/2}(\text{Na}_{0.82}\text{K}_{0.18})_{1/2}\text{TiO}_3$ lead-free ceramics", *J. Appl. Phys.*, Vol. 113, No. 15, pp. 154102(1)-154102(6), 2013.
- [45] X. X. Sun, J. Zhang, X. Lv, X. X. Zhang, Y. Liu, F. Li, and J. Wu, "Understanding the piezoelectricity of high-performance potassium sodium niobate ceramics from diffused multi-phase coexistence and domain feature", *J. Mater. Chem. A*, Vol. 7, No. 28, pp. 16803-16811, 2019.